Geophys. J. Int. (2000) **141,** 809–819

Magnetic properties of hydrothermally synthesized greigite (Fe_3S_4)—II. High- and low-temperature characteristics

Mark J. Dekkers,[1] Hilde F. Passier[1] and Martin A. A. Schoonen[2]

[1] *Palaeomagnetic Laboratory 'Fort Hoofddijk', Institute of Earth Sciences, Universiteit Utrecht, Budapestlaan* 17, 3584 CD *Utrecht, The Netherlands. E-mail: dekkers@geo.uu.nl*

[2] *Department of Geosciences, State University of New York at Stony Brook, Stony Brook,* NY 11794–2100, *USA*

Accepted 2000 February 1. Received 2000 February 1; in original form 1999 July 25

SUMMARY

The magnetic behaviour of hydrothermally synthesized greigite was analysed in the temperature range from 4 K to 700 °C. Below room temperature, hysteresis parameters were determined as a function of temperature, with emphasis on the temperature range below 50 K. Saturation magnetization and initial susceptibility were studied above room temperature, along with X-ray diffraction analysis of material heated to various temperatures. The magnetic behaviour of synthetic greigite on heating is determined by chemical alteration rather than by magnetic unblocking. Heating in air yields more discriminative behaviour than heating in argon. When heated in air, the amount of oxygen available for reaction with greigite determines the products and magnetic behaviour. In systems open to contact with air, haematite is the final reaction product. When the contact with air is restricted, magnetite is the final reaction product. When air is excluded, pyrrhotite and magnetite are the final reaction products; the amount of magnetite formed is determined by the purity of the starting greigite and the degree of its surficial oxidation. The saturation magnetization of synthetic greigite is virtually independent of temperature from room temperature down to 4 K. The saturation remanent magnetization increases slowly by 20–30 per cent on cooling from room temperature to 4 K. A broad maximum is observed at ~10 K which may be diagnostic of greigite. The coercive and remanent coercive force both increase smoothly with decreasing temperature to 4 K. The coercive force increases from ~50 mT at room temperature to approximately 100–120 mT at 4 K, and the remanent coercive force increases from approximately 50–80 mT at room temperature to approximately 110–180 mT at 4 K.

Key words: alteration, greigite, hydrothermal synthesis, magnetic properties.

1 INTRODUCTION

Greigite (Fe_3S_4) was first defined as a mineral by Skinner *et al.* (1964), who found it in a lacustrine sediment sequence from California. Since then, despite the fact that greigite has a limited stability with respect to pH and dissolved sulphur activity (Garrels & Christ 1965; Berner 1967), it has been identified in many natural environments of up to a few million years old (sediments: Snowball & Thompson 1988; Krs *et al.* 1990, 1992; Snowball 1991; Horng *et al.* 1992a, 1992b; Roberts & Turner 1993; Hallam & Maher 1994; Florindo & Sagnotti 1995; Roberts 1995; Roberts *et al.* 1996; Torii *et al.* 1996; Horng *et al.* 1999; Sagnotti & Winkler 1999; Roberts *et al.* 1999; soils: Fassbinder & Stanjek 1994). Older greigite is described by Reynolds *et al.* (1994), who speculate on early diagenetic greigite of Cretaceous age. Krupp (1994) described hydrothermal greigite formed under low-temperature conditions, which supposedly would have an age of ~280 Ma. Recently, greigite has become easier to identify, largely because rock-magnetic criteria have been developed that aid in its detection (e.g. Snowball & Thompson 1990; Roberts 1995; Dekkers & Schoonen 1996; Snowball 1997; Snowball & Torii 1999). Furthermore, the awareness that greigite may alter during storage has contributed to its identification (Snowball & Thompson 1990; Oldfield *et al.* 1992).

Despite the increased recognition of greigite in some environments, the rock-magnetic properties of greigite are not yet known in detail, and the stability of greigite in stored samples is ambiguous. Changes in magnetic properties due to oxidation in wet samples have been used to suggest the presence of greigite (e.g. Snowball & Thompson 1990). However, there are also cases where greigite has survived storage for long periods,

particularly when the samples were dry (Reynolds *et al.* 1994; Roberts *et al.* 1996). In one of these cases, the greigite survived storage for 50 years (Reynolds *et al.* 1994). In addition, susceptibility loss during drying can indicate the presence of magnetite as well as of greigite in the original samples (Oldfield *et al.* 1992).

An investigation into the magnetic properties of greigite will provide further tools for identifying the presence of greigite in natural samples, even when it occurs in trace amounts. Knowledge of the minerals that carry a stable natural remanent magnetization (NRM) is crucial for palaeomagnetic applications to tectonics, geochronology, and geomagnetic field behaviour. Greigite can be formed diagenetically after deposition of sediments during bacterial sulphate reduction (e.g. Reynolds *et al.* 1994), or in the presence of hydrothermal fluids (e.g. Krupp 1994). Therefore, the age of greigite and the chemical remanent magnetization (CRM) that it carries are not necessarily the same as those of the hosting sediments or rocks. Dekkers & Schoonen (1994, 1996) investigated electrokinetic mobility and rock-magnetic properties of greigite at room temperature. This greigite was synthesized by a hydrothermal method. The present contribution focuses on the magnetic behaviour of the synthetic greigite from $-269\,^{\circ}C$ (4 K) up to 700 °C. We finish by presenting a procedure to identify greigite by magnetic means.

1.1 Physical properties of greigite

Greigite is the ferrimagnetic inverse thiospinel of iron. It has localized valence electrons, as opposed to linnaite (Co_3S_4), polydymite (Ni_3S_4), carrolite ($CuCo_2S_4$) and violarite ($FeNi_2S_4$) (Vaughan & Craig 1985; Vaughan & Tossel 1981). The latter four thiospinels have delocalized valence electrons, which result in metallic conductivity and Pauli paramagnetism (i.e. temperature-independent paramagnetism). Their unit cells [9.40, 9.42, 9.46 and 9.53 Å, respectively, see Vaughan & Craig (1976)] are smaller than that of greigite (9.876 Å). Electron hopping is inferred to occur between high-spin ferric and ferrous iron in octahedral lattice positions in greigite (Coey *et al.* 1970), a property that could result in metallic conductivity. Molecular orbital calculations have shown that the octahedral lattice positions contain mixed ferric and ferrous iron (Vaughan & Tossel 1981; Vaughan & Craig 1985). Spender *et al.* (1972) determined the conductivity of greigite to be 'semimetallic', and attributed non-stoichiometry to Fe-vacancies on the octahedral lattice sites. Vaughan & Craig (1985) argued that, on account of their different electronic structures, there is no stable solid solution between greigite and the nickel-bearing thiospinels. They showed intermediate compositions identified by electron microprobe analysis, but related these either to metastability or to preferential alteration of pentlandite to violarite, a common violarite formation pathway.

Greigite particles that are identified by X-ray diffraction are usually pure without significant substitution (e.g. Roberts 1995). Magnetic hysteresis measurements of sedimentary greigite and the occurrence of gyroremanent magnetization during alternating field demagnetization indicate a dominant single domain state (e.g. Snowball 1991; Roberts 1995; Snowball 1997; Hu *et al.* 1998). Larger grains are described in low-temperature ores (Krupp 1994) and Miocene coal beds in the Czech Republic (Krs *et al.* 1990). Synthetic greigite is usually more fine-grained than natural greigite (e.g. Snowball & Torii 1999). The greigite used in the present study has a grain size of between ~200 and 300 nm (ranging from <150 to 400 nm; Dekkers & Schoonen 1996), which belongs to the largest greigites synthesized to date.

1.2 Thermomagnetic behaviour of greigite

During thermomagnetic analysis in air (applied fields $> \sim 0.1$ T), greigite shows a typical drop in magnetization between ~250 and ~350 °C (e.g. Snowball & Thompson 1988, 1990; Snowball 1991; Horng *et al.* 1992b; Roberts & Turner 1993; Reynolds *et al.* 1994; Roberts 1995). This decrease in magnetization is caused by the alteration of greigite to sulphur, pyrite, marcasite and pyrrhotite (Skinner *et al.* 1964; Krs *et al.* 1992). Further oxidative alteration, starting at approximately 400 °C, yields magnetite in natural samples, as can be deduced from an increase of magnetization in thermomagnetic runs in air. Haematite is the ultimate oxidation product on heating at 600° to 700 °C in air (Krs *et al.* 1992). In a nitrogen or argon atmosphere, the typical thermal alteration is less pronounced (e.g. Snowball & Thompson 1990), a fact which led Reynolds *et al.* (1994) to recommend heating in air to identify greigite in sediments and sedimentary rocks. Synthetic greigite is generally more fine-grained than natural greigite, and is expected to react at lower temperatures during heating than natural greigite.

For synthetic greigite, Coey *et al.* (1970) inferred a Néel (or Curie) temperature of $297 \pm 8\,^{\circ}C$ from a thermal scan of remanent magnetization. Spender *et al.* (1972), also for synthetic greigite, inferred a higher Curie temperature of 333 °C, which is more consistent with data for natural greigite. Van den Berghe *et al.* (1991), however, found a Curie temperature of 527 °C based on extrapolation of their temperature-dependent Mössbauer measurements. This observation implies that thermal decomposition of greigite—of either synthetic or natural origin—precludes meaningful direct measurement of its Curie temperature. Therefore, claims of a 'Curie temperature' for greigite should be regarded with caution, as already argued for by Roberts (1995) and Snowball & Torii (1999). Torii *et al.* (1996) analysed the magnetic behaviour of isothermal remanent magnetization (IRM) residing in pyrrhotite- and greigite-bearing sediments. They reported that greigite alters chemically on heating, with thermal decomposition starting at approximately 200 °C.

1.3 Low-temperature behaviour of greigite

On cooling to 4 K, greigite, synthetic or natural, does not show a magnetic transition similar to the Verwey transition in magnetite (Spender *et al.* 1972; Moskowitz *et al.* 1993; Roberts 1995; Torii *et al.* 1996). Spender *et al.* (1972) also report no discontinuity in the temperature dependence of the electrical conductivity of synthetic greigite on cooling. The reason for the absence of a low-temperature transition is unclear at present.

2 MATERIAL AND METHODS

Greigite was synthesized by injecting a Mohr's salt solution into a sodium sulphide solution containing zerovalent sulphur at 140 °C [molar S(-II)/S(0) ratio equal to 3:1; Dekkers & Schoonen 1994, 1996]. The rock-magnetic data were collected

on the same greigite and in the same period as the data published by Dekkers & Schoonen (1994, 1996). In addition, fresh greigite synthesized according to the same recipe was used for X-ray diffraction (XRD) analysis. All samples were stored in a desiccator.

Thermomagnetic runs in air (samples EXP28, EXP30, G932, G934) and in argon (G932, G934) were carried out with a modified horizontal-translation-type Curie balance with a sensitivity of approximately 5×10^{-9} A m^2 (Mullender *et al.* 1993). A few milligrams of greigite powder were put into a quartz glass sample holder and were held in place by quartz-wool. Heating and cooling rates were 10 °C min^{-1}. For runs in an argon atmosphere, the sample holder was purged with argon before it was suspended in the Curie balance; a laminar flow ($\sim$3 cm^3 min^{-1}) of argon was maintained in the furnace.

The thermal behaviour of the low-field or initial susceptibility (χ_{in}) was measured with a CS-2 heating unit attached to an AGICO KLY-2 susceptibility bridge on $\sim$50 mg samples at the Institute for Rock Magnetism (University of Minnesota, USA). EXP28 and G932 were measured in air and in argon. The sample was placed at the closed end of a 15-cm-long glass tube with a diameter of 3 mm, so that the contact with air was limited. During the runs in argon, the sample was continuously flushed at a flow rate of $\sim$3 cm^3 min^{-1}. The heating and cooling rates were comparable to those used in the Curie balance measurements.

Hysteresis measurements (samples EXP26, EXP28, EXP31, EXP33, EXP34b, G932, G935) below room temperature were done with a Princeton Applied Research vibrating sample magnetometer equipped with a helium cryostat, at Nijmegen University (The Netherlands) in the autumn of 1993. The maximum field was 1.2 T. The saturation magnetization (M_s per unit volume or σ_s when expressed per unit mass), remanent saturation magnetization (M_{rs} or σ_{rs}), coercive force [$(B_0)_c$] and remanent coercive force [$(B_0)_{cr}$] were determined at a substantial number of temperatures, in particular at temperatures $<$50 K. The samples were subjected to a 1.2 T field at room temperature, and were subsequently cooled to 4 K in a $<$1 μT field in order to study the behaviour of σ_{rs} induced at room temperature. Starting at 4 K, the hysteresis parameters were measured, which took approximately 20 min at each temperature; the desired field values were set manually. Thereafter, the sample was warmed to the next temperature, the hysteresis parameters measured once more, and so forth. For these low-temperature measurements, 1–11 mg of greigite was dispersed in 35 mm^3 of epoxy resin; that is, 0.7–7 per cent by volume assuming 100 per cent purity and a density of 4080 kg m^{-3} (Skinner *et al.* 1964).

Samples for X-ray diffraction analysis (S15998, S16798, S81098, S21798) of the greigite alteration products were prepared in the following three ways. (1) Greigite (0.5–5 mg) was heated and cooled (10 °C min^{-1}) in the Curie balance, in contact with air. (2) Greigite ($\sim$50 mg) was heated in an oven in air in open porcelain dishes for 1 hr at the desired temperature, and then cooled inside a desiccator. (3) Greigite (10–30 mg) was heated and cooled ($\sim$10 °C min^{-1}) in a CS-3 heating attachment to an AGICO KLY-3 susceptibility bridge. The furnace tube was closed to air inflow and the maximum temperature was maintained for 20 min. After heating, samples for X-ray diffraction were prepared by mounting the grains on glass plates with silica grease. Diffractograms were recorded on a Philips PW1700 instrument (CuK_α, stepscan 0.02° 2Θ, counting time 1 s per increment).

3 RESULTS

3.1 Thermomagnetic analysis

All strong-field thermomagnetic curves (referred to as Curie curves) measured in air show an irreversible decrease in magnetization with increasing temperature, starting at around 200 °C; at 350 °C this decrease is complete (Fig. 1). Relevant data are compiled in Table 1. Before thermomagnetic analysis, σ_s differs among the samples, which indicates a variable purity of the synthesis products. Samples with the lowest σ_s are considered to be the least pure. This low σ_s could be a consequence of the presence of pyrite in addition to greigite as identified by XRD analysis. The possibility that some material is X-ray-amorphous, that is $<$100 nm in size, cannot be excluded. Repeated measurement after 8 months showed a 25 per cent decrease in σ_s for sample G934. The thermomagnetic signal decays more rapidly with increasing temperature in samples with a higher initial σ_s. This can be deduced from the temperature at which σ_s is half its initial value ($T_{1/2}$; Fig. 1, Table 1); the sample with the highest initial σ_s has the lowest $T_{1/2}$. After the 450°, 600° and 700 °C runs in air, the sample material was a reddish colour, which indicates the presence of haematite and/or maghemite. σ_s at room temperature after the 450° and 600 °C runs is $\sim$1–2 A m^2 kg^{-1}, which is too high for pure haematite. In other thermomagnetic runs (not shown here), the presence of maghemite could be inferred from Curie temperatures of $\sim$630 °C during heating to 700 °C. Those Curie temperatures were not visible on the cooling curves, which indicates that conversion to haematite occurred. Magnetite ($T_C \sim 580$ °C) was also noticeable as an intermediate phase (Fig. 1). In the 700 °C run, haematite can be inferred from its Curie temperature at $\sim$680 °C (Fig. 1a).

The Curie curves measured in argon are distinctly different from those in air. When greigite is heated in argon (Fig. 2), the Curie curves are more reversible from room temperature to 600 °C. Just above 200 °C there is a slight inflection that is visible even after the fifth heating cycle (Fig. 2). After heating to 450 °C and 550 °C, a Curie temperature of approximately

Table 1. $T_{1/2}$ for several greigite samples.

Thermomagnetic Run, atmosphere	sample	Sto[1] (m.a.s)	$\sigma_s RT^2$[2] (A m^2 kg^{-1})	$T_{1/2}$[3] (°C)
Air	EXP26	14	17.5	244
Air	EXP28	18	29.2	243
Air	EXP28	26	29.2	243
Air	EXP30	18	17.7	255
Air	G934	6	13.1	243
Air	G934	17	9.8	251
Air	G932	6	4.9	276
Argon	G932	6	4.9	370
Argon	G934	6	13.1	396

[1] Storage in months after synthesis. [2] $\sigma_s RT$ is the saturation magnetization at room temperature. [3] $T_{1/2}$ is the temperature at which the magnetization reaches half its starting value, as determined from thermomagnetic runs in air or argon for several greigite samples.

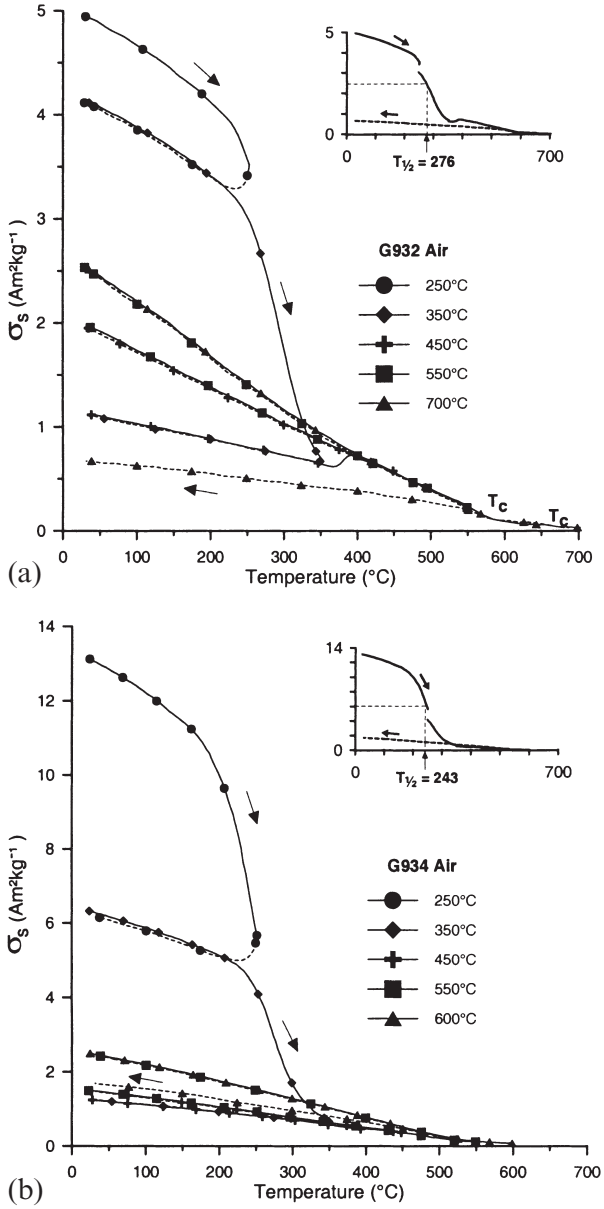

Figure 1. Thermomagnetic analysis of synthetic greigite in air with the modified horizontal translation Curie balance (Mullender *et al.* 1993), with field cycling between 200 and 300 mT, and heating and cooling rates of 10 °C min^{-1}. (a) Sample G932, (b) Sample G934. Saturation magnetization (σ_s) is plotted in a series of runs to increasingly higher temperatures. Heating curves are indicated by solid lines, cooling curves by dashed lines. Each 15th data point is indicated by a symbol. Arrows refer to heating and cooling segments, respectively. Curie temperatures are indicated by T_C. $T_{1/2}$ is the temperature at which the magnetization has dropped to 50 per cent of its starting value. The insets show the corresponding 'composite' runs, i.e. as if one heating cycle to the maximum temperature was performed. These are constructed from the heating curves of the segmented runs and the cooling curve of the last run.

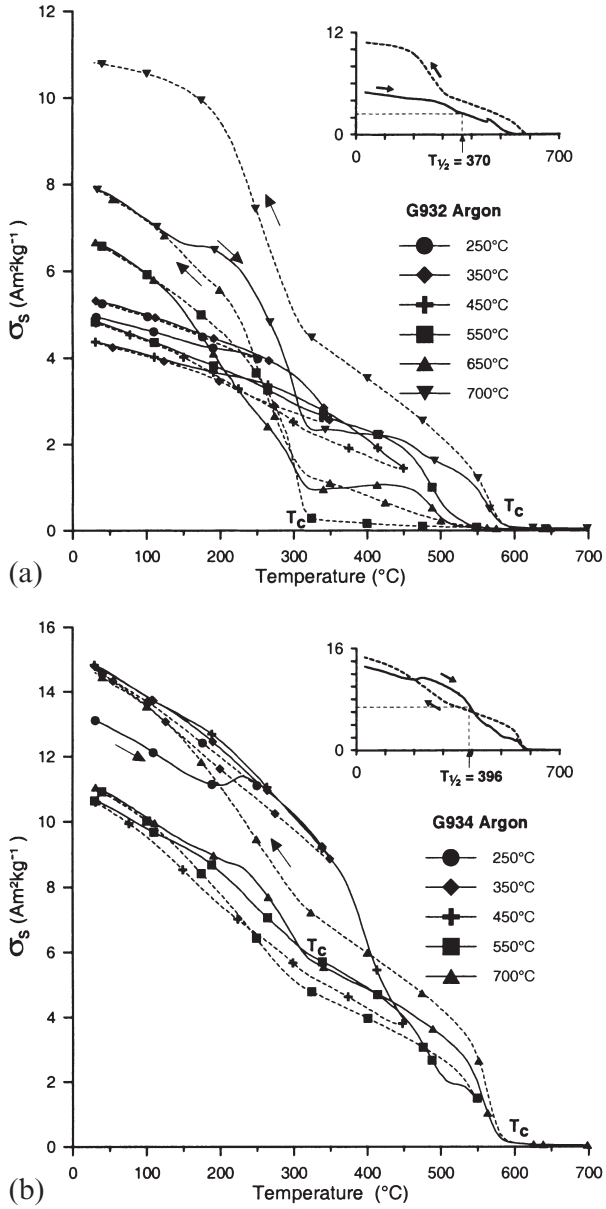

Figure 2. Thermomagnetic analysis in argon of samples (a) G932 and (b) G934. See the caption of Fig. 1 for explanation of instrument settings and line appearances. Note the marked differences in thermomagnetic behaviour as a function of atmosphere and sample purity as inferred from the σ_s values.

325 °C is evident, which suggests that pyrrhotite has formed (e.g. Schwarz 1975). In contrast to the measurements in air, the argon runs indicate that the sample with the highest initial σ_s has the highest $T_{1/2}$ (Table 1). Heating in argon to 550°, 650°, and 700 °C produces progressive formation of a compound with a Curie temperature of ~580 °C, namely magnetite. Its formation is also visible from sharp changes in magnetization at ~550 °C, during cooling of the 550 °C run and during heating in the 650 °C run. The formation of magnetite continues above 580 °C, but, during cooling, pyrrhotite is still present. After heating to 700 °C, pure magnetite has formed, as characterized by a Curie temperature of 580 °C and a smooth thermomagnetic curve. Graham *et al.* (1987) attributed similar observations of magnetite-like behaviour to small amounts of oxygen that can dissolve in pyrrhotite and which give rise to remarkable irreversible thermomagnetic behaviour between 400° and 600 °C. Graham *et al.* (1987) argue that only sufficiently large amounts of oxygen would result in the formation of pure magnetite with a Curie temperature of 580 °C.

3.2 High-temperature dependence of χ_{in}

The behaviour of χ_{in} on heating in air is also characterized by thermal alteration (Fig. 3). Alteration sets in at ~200 °C for EXP28 (Fig. 3a) and at ~250 °C for G932 (Fig. 3b). After heating to 350 °C, the sample has a lower χ_{in} at room temperature than before heating. During heating to above ~400 °C for EXP28 and above 440 °C for G932, a new magnetic phase has formed as indicated by an increase of χ_{in}. This phase continues to form during cooling. The behaviour of χ_{in} during heating to 600 °C for EXP28 or 650 °C for G932 (Fig. 3) is clearly dominated by magnetite (T_C ~ 580 °C).

In an argon atmosphere, χ_{in} is almost reversible up to 350 °C (Fig. 4). In EXP28, detectable alteration starts at ~360 °C. A discontinuity occurs at ~310 °C on the cooling curve of the 450 °C run: this feature remains after heating to 600 °C and is probably due to the formation of pyrrhotite. It is difficult to identify pyrrhotite in thermal scans of χ_{in}, presumably because differences in χ_{in} values among reaction products are not large, with, of course, the notable exception of magnetite, which formed in both EXP28 and G932. In G932, the 'hump' at ~240 °C in the cooling curve of the 650 °C run could possibly indicate the presence of anomalous pyrrhotite or smythite. Both of these phases are oxidation products of pyrrhotite

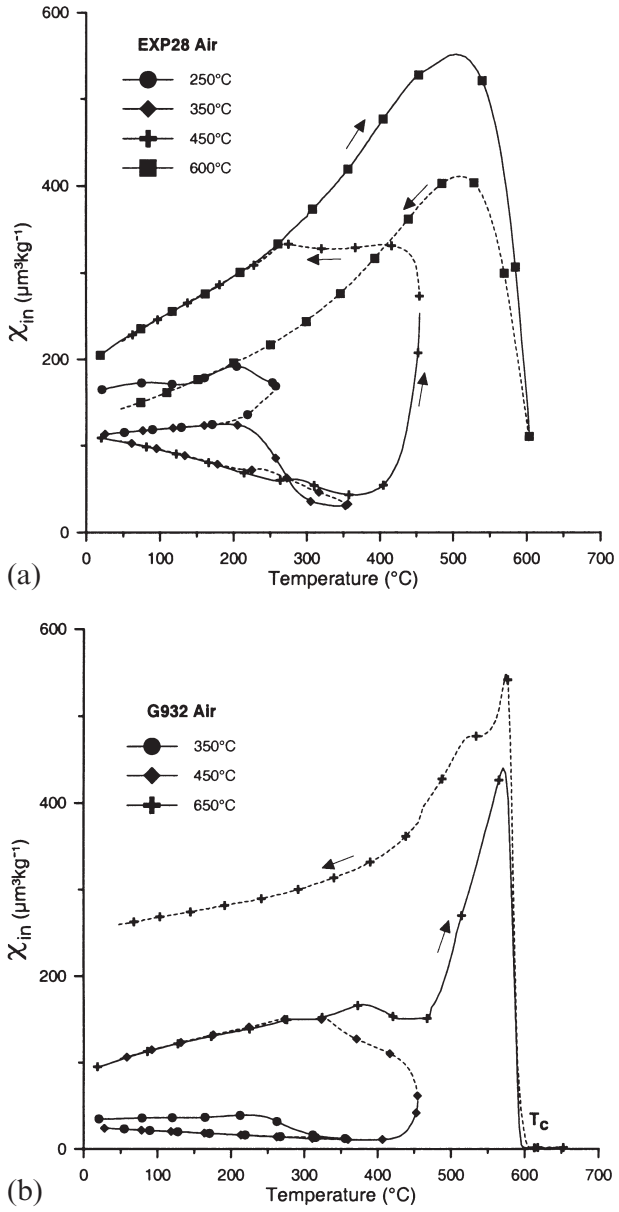

Figure 3. Low-field susceptibility (χ_{in}) as a function of temperature measured in 'air' for sample (a) EXP28 and (b) G932. Measurements were carried out with a CS-2 heating unit attached to a KLY-2 susceptibility bridge. Heating curves are indicated by solid lines, cooling curves by dashed lines. Each 15th data point is shown, and arrows indicate heating and cooling, where appropriate. The behaviour of χ_{in} is difficult to quantify in terms of concentration of magnetic phases because the curves are quickly dominated by magnetite which forms on heating. T_C refers to the Curie temperature where it could be determined.

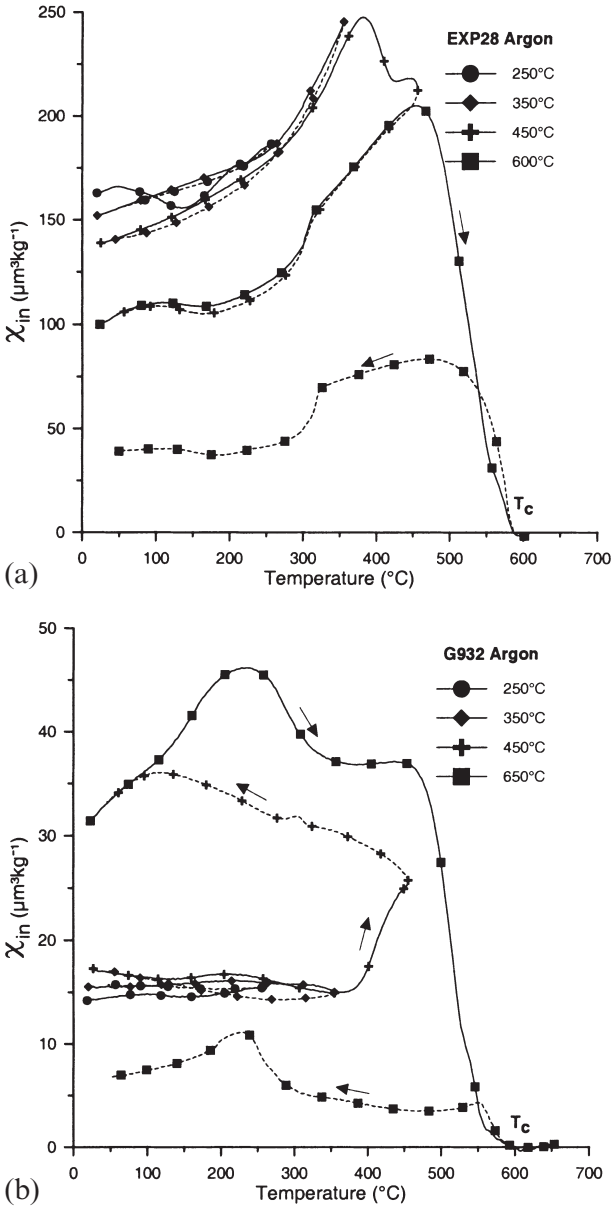

Figure 4. χ_{in} as a function of temperature in argon for sample (a) EXP28 and (b) G932. Lines and symbols are as in Fig. 3. The magnetically detectable heating products are magnetite and pyrrhotite.

with upper stability limits of ~250 °C, characteristic of the initial oxidation stage (see Taylor 1970; Taylor & Mao 1971). Magnetite was also formed during heating in both experiments, as deduced from a T_C of ~580 °C. After a sequence of runs the powder was black, and a yellow crust, possibly elemental sulphur, was precipitated on the glass tube a few centimetres above the sample, where the furnace is cooler.

3.3 XRD analysis of high-temperature products

The black greigite powders heated in the Curie balance changed colour to reddish/orange, and the Curie curves clearly indicate oxidation to iron oxides as a function of temperature. The crystallite size of these oxides must be very small (< 100 nm), however, because the X-ray diffractograms do not show clear reflections at the expected peak positions. The small crystallites probably result from the absence of a dwell time at the maximum heating temperature. The products of heating in an oven, open to air with a dwell time of 1 hr, as well as heating in the CS3 attachment, closed to air with a dwell time of 20 min, give X-ray diffractograms with clear iron oxide reflections (Table 2). The products have very distinct differences in colour, which are similar to the colours expected for iron oxides (Schwertmann & Cornell 1991). Greigite changes to pyrite after heating to 350 °C, both in the oven and in the CS3 attachment. In the oven, oxidation produces magnetite/maghemite at 450 °C. The colour of the product is red-brown (i.e. maghemite). It is, however, difficult to distinguish between magnetite and maghemite by XRD. The X-ray reflections after heating at 450 °C are distinctly broader than those of pyrite after heating at 350 °C, which indicates a smaller crystallite size of the spinel phase at 450 °C. Subsequently, well-crystalline red-orange haematite forms after heating to 600 °C. In the CS3 attachment, which is closed to air, pyrite remains the dominant phase up to 450 °C, and pyrrhotite is dominant at 600 °C.

3.4 Low-temperature behaviour of greigite

On cooling to 4 K, σ_{rs} induced at room temperature is virtually independent of temperature (Fig. 5). This observation concurs with that made for natural greigite and other synthetic greigite samples (Spender *et al.* 1972; Moskowitz *et al.* 1993; Roberts 1995; Torii *et al.* 1996). The values of σ_s, σ_{rs} $(B_0)_c$ and $(B_0)_{cr}$ as a function of temperature are shown in Figs 6(a) to (d). These parameters were obtained from hysteresis loops measured at each temperature. σ_s is virtually independent of temperature,

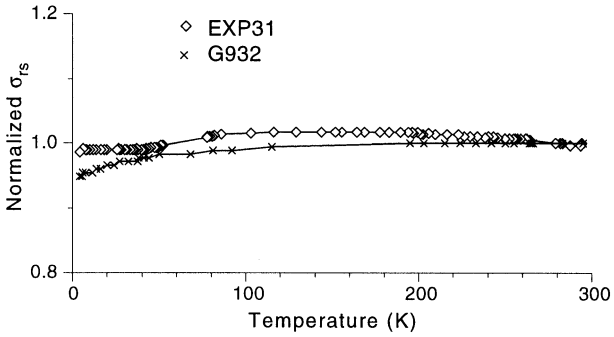

Figure 5. Behaviour of σ_{rs} for synthetic greigite induced at room temperature on zero-field cooling to 4 K, normalized to its initial value. Sample EXP31 was stored for ~22 months before the measurements, whereas sample G932 was a 'fresh' sample.

whereas σ_{rs} gradually increases with decreasing temperature to a maximum value at ~10 K, below which a small decrease is observed. The σ_{rs} maximum at ~10 K in sample G932 is small (see also Fig. 7), while that in G935 is more prominent. This may be related to the low value of σ_s at room temperature for the former sample (4.9 A m^2 kg^{-1} for G932 versus 13.3 A m^2 kg^{-1} for G935). $(B_0)_c$ and $(B_0)_{cr}$ also increase with decreasing temperature. Below ~40 K, the increase with decreasing temperature for both parameters is larger than above this temperature. Values of $(B_0)_c$ tend to ~110 mT at 4 K for all samples except G932 (~80 mT). Sample G932 is considerably less pure, which presumably indicates a smaller average grain size than for the other samples. $(B_0)_{cr}$ values at 4 K are less convergent; G932 has a notably lower coercivity than the other samples, again hinting at a smaller grain size.

4 DISCUSSION

4.1 Thermal alteration products of greigite

4.1.1 Pyrite

XRD results indicate that pyrite is the first major alteration product of greigite above room temperature, either when heated in air or in an inert atmosphere (Table 2). In addition, small amounts of marcasite were found. Krs *et al.* (1992) observed the same products for natural greigite. Pyrite converts to pyrrhotite and sulphur on heating to ~550–600 °C in inert

Table 2. XRD analysis of thermal alteration products of synthetic greigite.

Sample	Device[1]	T (°C)	Product colour	Dominant mineral	Additional minerals
S15998	Oven	250	Black	Pyrite	Marcasite, Greigite
S15998	Oven	350	Brownish-black	Pyrite	Marcasite
S15998	Oven	450	Red-brown	Maghemite/Magnetite	
S15998	Oven	600	Red-orange	Haematite	
S16798	CS-3	250	Black	Pyrite	Greigite
S15998	CS-3	350	Black	Pyrite	Greigite
S81098	CS-3	450	Black	Pyrite	Pyrrhotite, Sulphur, Greigite
S81098	CS-3	600	Black	Pyrrhotite	Pyrite, Jarosite, Maghemite/Magnetite

[1] The oven was open to air. The CS-3 attachment was closed to air. XRD measurements on greigite heated in air in the Curie balance yielded broad peaks that were mostly not identifiable. Some pyrite peaks could be identified, however, after heating to 250 and 350 °C. Haematite peaks were present after heating to 600 °C.

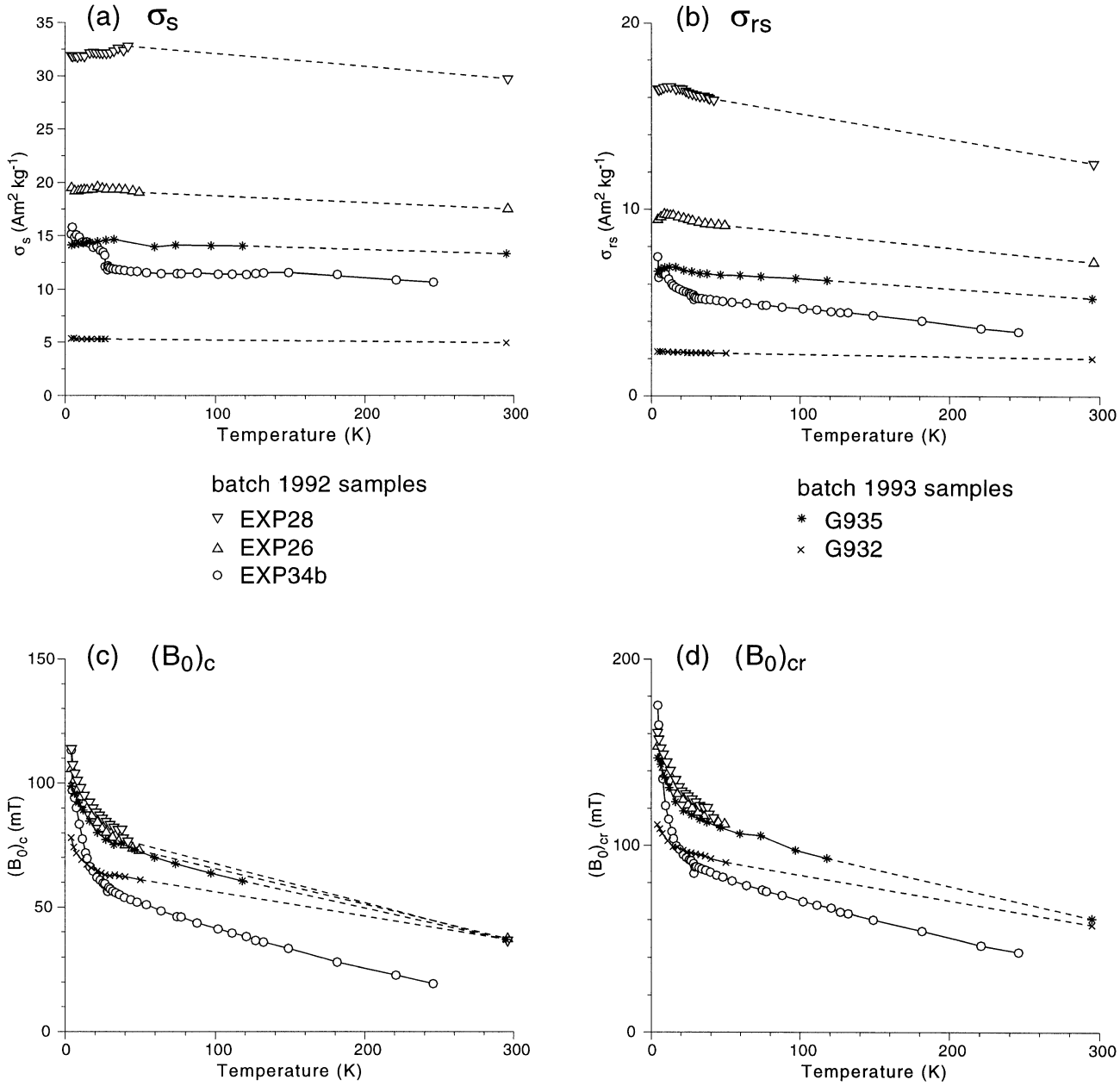

Figure 6. Hysteresis parameters as a function of temperature for the synthetic greigites. Samples EXP26, EXP28 and EXP34b were stored for ~22 months before the measurements, whereas amples G932 and G935 were 'fresh' samples. The parameters were acquired from hysteresis loops acquired at the temperatures indicated, measured from 4 K upwards. (a) Saturation magnetization σ_s (induced in a 1.2 T field); (b) remanent saturation magnetization σ_{rs}; (c) coercive force $(B_0)_c$; and (d) remanent coercive force $(B_0)_{cr}$.

atmospheres, depending on the crystal size (Hoare *et al.* 1988). In air, pyrite oxidizes to magnetite and finally to haematite (e.g. Krs *et al.* 1992).

4.1.2 Pyrrhotite

Greigite has been reported to convert to pyrrhotite and pyrite or to pyrrhotite and sulphur on heating in air (e.g. Skinner *et al.* 1964; Krs *et al.* 1992). Thus, pyrrhotite may be formed from greigite either directly or via pyrite (Skinner *et al.* 1964; Hoare *et al.* 1988; Krs *et al.* 1992). Our thermomagnetic runs in air do not allow the determination of the presence of pyrrhotite in the chain of oxidation reactions because its Curie temperature falls in the range where most alteration occurs. It may, however, be present as a transient phase that quickly oxidizes. When heated in argon, pyrrhotite was detected by XRD and in thermomagnetic runs in the Curie balance. It started forming between 350° and 400 °C, that is at temperatures higher than in the experiments of Skinner *et al.* (1964). The experiments of Skinner *et al.* (1964) refer to heating for over 10 hr, and, as they note, prolonged heating at a low temperature may be equivalent to shorter heating at a higher temperature for kinetic reasons. Our results are based on experiments in which the heating duration is considerably shorter, which explains the higher alteration temperatures. Pyrrhotite was the major constituent after heating to 600° and

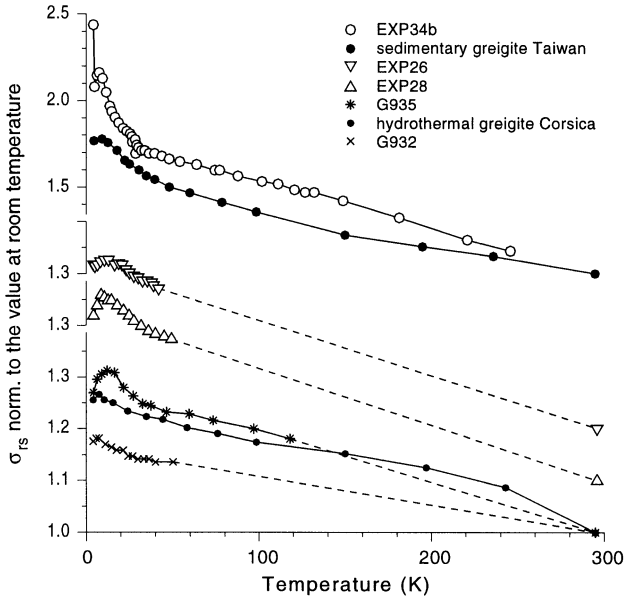

Figure 7. Remanent saturation magnetization σ_{rs} normalized to its value at room temperature for the synthetic greigites and some natural greigites, measured according to the procedure of Fig. 6. The natural greigite samples are indicated with full circles: the upper curve (large full circles) is a sedimentary greigite sample from Taiwan (see Horng *et al.* 1992a), and the lower curve (small full circles) is a hydrothermal greigite sample from Corsica. Increased values at low temperatures are due to increased blocking of smaller particles with decreasing temperature. σ_{rs} shows a maximum at $\sim$10 K which could be typical of greigite. Natural greigite from various locations shows the same behaviour.

650 °C (XRD, thermomagnetic analysis), and it remained present after heating to 700 °C, as indicated by the persistent Curie temperature of 325 °C.

4.1.3 Magnetite and maghemite

Magnetite and maghemite are present after heating greigite in argon and in air above $\sim$400 °C. They are visible in magnetic observations and XRD results (Figs 2 and 4, Table 2). Formation of these iron oxides in an inert atmosphere indicates that some oxygen must have sorbed onto the original greigite surface during storage. Maghemite does not survive heating to 700 °C.

4.1.4 Haematite

Haematite is the final product of oxidation in air on heating to 700 °C, as indicated by thermomagnetic runs and XRD results (Fig. 1, Table 2). Moreover, after heating, the sample material has the red-orange colour typical of haematite (Schwertmann & Cornell 1991). Haematite could easily escape detection in χ_{in} versus temperature runs (Fig. 3), because the χ_{in} of magnetite is two to three orders of magnitude higher than that of haematite (room temperature values, Collinson 1983; Hunt *et al.* 1995). Haematite, however, probably did not form during the χ_{in}–temperature experiments that are closed to air, as the magnetite signal remains present, at least to a large extent. Furthermore, after the experiment, the powder was black rather than red.

4.1.5 Comparison of thermal scans of χ_{in} and thermomagnetic analysis in the Curie balance

It is easier to derive quantitative information from thermomagnetic runs than from thermal scans of χ_{in}, because the differences in σ_s values below the Curie temperature and paramagnetism above the Curie temperature are usually more evident (with the notable exceptions of magnetite and maghemite). χ_{in}–temperature data, however, may show more subtle variations, which yield valuable information for the interpretation of (incipient) alteration processes. Unfortunately, because of their high χ_{in} values, magnetite and/or maghemite dominate other magnetic minerals. This limits the value of χ_{in} versus temperature runs for quantification purposes. When dealing with fine-grained magnetic sulphides, variations in crystallinity and variations in surficial oxidation add to the complexity of the interpretation of χ_{in}–temperature measurements.

4.2 Greigite storage and impurity

4.2.1 Low-temperature data

The fine-grained synthetic greigite appears to alter slowly with time, despite storage under dry conditions in a desiccator. This becomes apparent from the changes in σ_s, as indicated by thermomagnetic runs repeated after 8 months (Table 1) and from the low-temperature data. The hysteresis parameters of freshly synthesized samples (G932 and G935) change less with decreasing temperature than those of the stored (18 months) samples (EXP26, EXP28 and EXP34b). The variation in σ_{rs}/σ_s and $(B_0)_{cr}/(B_0)_c$ with temperature of the freshly synthesized samples is distinctly less than that in the stored samples (see the 'Day' plot in Fig. 4 of Dekkers & Schoonen 1996). Apparently, (incipient) alteration has resulted in the presence of a wider grain-size spectrum in the ultrafine grain-size realm, as emerges from their higher $(B_0)_{cr}/(B_0)_c$ values of >2 versus $\sim$1.6 for the fresh samples (see Dekkers & Schoonen 1996). EXP34b shows a deviating behaviour which may be related to the presence of elemental sulphur and pyrite, which were detected by XRD in addition to greigite (Dekkers & Schoonen 1996). Elemental sulphur and pyrite were not detected in EXP26 and EXP28 (Dekkers & Schoonen 1996). The distinctly altered sample EXP34b shows a sharper increase in hysteresis parameters at low temperatures than the other samples, in particular an increase of $(B_0)_c$ and $(B_0)_{cr}$ values. The trend in the $(B_0)_c$ data of Spender *et al.* (1972) is similar to the observations made for the stored samples. Their greigite may therefore also have been partially altered. Analysis of the magnetic behaviour below room temperature yields clearer insight into the subtleties of incipient alteration than X-ray methods. XRD analysis of the distinctly altered sample EXP34b showed pyrite and S_0. Neither Fe-enriched sulfidic material nor iron oxides are observed, which is at odds with expectations for material of nominal Fe_3S_4 composition (partially) altering to FeS_2 and S_0. Presumably, X-ray-amorphous material is also formed in the alteration process. The distinctly altered sample EXP34b shows a discontinuity in the σ_s versus temperature trend at $\sim$30 K which is absent in the other samples. This discontinuity may hint at the presence of pyrrhotite.

4.2.2 Surficial oxidation of greigite

Electrokinetic mobility measurements (Dekkers & Schoonen 1994) indicate a sulphidic (i.e. reduced) surface layer for the greigite particles (zeta potential as a function of pH is different from pyrrhotite and from elemental sulphur), but minor oxidation as a consequence of imperfect synthesis conditions or storage cannot be excluded. Oxidation progresses from the rims to the cores of the greigite particles. Although surface oxidation processes have not yet been studied specifically for greigite, much work in this field has been done on pyrrhotite and pyrite. This work is summarized briefly below and provides a basis for the interpretation of the greigite behaviour.

An important outcome of the surface oxidation studies on pyrrhotite and pyrite is that both an oxidant (oxygen) and water are required to tarnish (oxidize) the surface of the sulphides (Knipe *et al.* 1995). The rims of oxidized pyrrhotite particles consist of an iron(oxy)hydroxide layer (0.5 nm) which is followed inwards by a pyritic layer with thiosulphate (3 nm thickness); this, in turn, is followed by non-altered pyrrhotite (Pratt *et al.* 1994; Mycroft *et al.* 1995). Fe migrates out of the sulphide crystal structure to form oxides at the rim. Growth of the oxide layer continues as long as there is an oxygen supply: diffusion of iron to the surface is considered to be the rate-limiting step in the reaction (Pratt *et al.* 1994). Another important aspect of the studies on pyrrhotite and pyrite is that pyrite is distinctly less reactive towards oxygen than pyrrhotite (Buckey & Woods 1985, 1987; Jones *et al.* 1992; Pratt *et al.* 1994; Knipe *et al.* 1995; Mycroft *et al.* 1995). Therefore, the pyritic layer could act as a protective barrier against further oxidation.

If these results can be extended to greigite, dry storage (removing water vapour) would limit surface oxidation to a large extent, which concurs with the observations of Reynolds *et al.* (1994) and of Roberts *et al.* (1996) and is in agreement with our observations. Furthermore, greigite would become progressively more resistant to oxidation after the formation of a pyrite shell resulting from the first oxidation stage. The pyritic layer could have been originally present (i.e. created during synthesis), or it could have formed during prolonged storage, or it could have formed at low temperatures during the thermomagnetic run. This would explain the slightly higher $T_{1/2}$ values for samples with a lower initial σ_s in thermomagnetic runs in air.

4.3 Thermal stability of greigite in different atmospheres

The thermomagnetic behaviour of the present synthetic greigite samples closely resembles that of natural (coarser-grained) greigite (e.g. Snowball & Thompson 1990; Roberts & Turner 1993; Reynolds *et al.* 1994). The diagnostic power of thermomagnetic behaviour for greigite detection is much larger in air—because of the typical oxidation reaction chain—than that in an inert atmosphere, and is therefore recommended (Reynolds *et al.* 1994; Roberts 1995). In the sample holder of the CS-2 (or CS-3) heating attachment, the powder is put at the closed end of a glass tube of $\sim$3 mm diameter and $\sim$15 cm length, which limits contact with surrounding air. Hence, the effective air/sample ratio is very different from that in the thermomagnetic runs. The thermal instability of fine-grained iron sulphide minerals requires that experimental conditions for the various instruments should be identical in order to be able to compare the results meaningfully. This necessitates either a vacuum, a truly inert atmosphere, or a specified supply of oxygen.

4.4 Low-temperature measurements

4.4.1 Absence of the Verwey transition

Synthetic and natural greigite are not reported to show a low-temperature transition (Spender *et al.* 1972; Moskowitz *et al.* 1993; Roberts 1995; Torii *et al.* 1996) like the Verwey transition of magnetite (e.g. Mott 1980) or the 34 K transition of pyrrhotite (Dekkers *et al.* 1989; Rochette *et al.* 1990; Fillion *et al.* 1992). The Verwey transition is a first-order transition at 115–120 K, below which the electrical conductivity is decreased by two orders of magnitude due to ordering of octahedral ferrous and ferric iron. Below the transition, the magnetite crystal structure becomes monoclinic rather than cubic. Associated with the transition is a magnetic isotropic point, and, on cooling through the transition, the easy direction in magnetite goes from the $\langle 111 \rangle$ to the $\langle 100 \rangle$ crystallographic direction (e.g. Özdemir *et al.* 1993). Marked changes in coercivity, susceptibility and remanence occur at the Verwey transition, which make the transition detectable by magnetic measurements. Non-stoichiometry suppresses the transition (e.g. Mott 1980; Aragón *et al.* 1985; Özdemir *et al.* 1993).

Following the suggestion by Mott (1980) for the apparent absence of a Verwey transition in Sm_3S_4, it could be that the available greigite samples are also not sufficiently stoichiometric to make a transition observable. Spender *et al.* (1972) concluded that there are vacancies in the greigite spinel structure, because Mössbauer spectra did not yield the expected intensity ratio of 1 : 2 of the spinel A and B sites. B-site vacancies would lead to the occurrence of localized FeS_2(-II); in other words, non-stoichiometry is induced. It could be that ongoing oxidation leads to a larger proportion of the material having the FeS_2(-II) localized configuration.

Available data on the electrical conductivity of greigite show no discontinuity (Spender *et al.* 1972), although Mössbauer spectroscopy at low temperatures shows splitting of the single sextet, which is typical of room-temperature measurements, into several sextets. Furthermore, in greigite, the $\langle 100 \rangle$ direction is suggested to be the easy direction in greigite at room temperature (Heywood *et al.* 1990), rather than $\langle 111 \rangle$ as in magnetite. This discontinuity in physical properties on cooling through a transition akin to the Verwey transition would not necessarily be observable by magnetic means in greigite.

4.4.2 Magnetic transition at $\sim$10 K?

In spite of the reported absence of a low-temperature transition in greigites, we observe a maximum in σ_{rs} versus temperature at $\sim$10 K (Fig. 6b). This maximum is most clearly visible in plots of σ_{rs} that are normalized to its value at room temperature (Fig. 7), and could be the result of a magnetic transition. Increased blocking of superparamagnetic (SP) grains with decreasing temperature as a consequence of a smaller SP threshold size would yield monotonously increasing σ_{rs} values (for increasingly finer grain-sizes). Furthermore, in the distinctly altered sample EXP34b, the normalized σ_{rs} curve has a maximum at $\sim$10 K which is superimposed on this increasing trend. This behaviour is observed in fresh as well as in stored

greigite and also in natural greigite of various provenances (Fig. 7). The natural sedimentary greigite from Taiwan has a particle size ranging from ~ 600 to ~ 1000 nm (Dekkers & Schoonen 1996), while the greigite of hydrothermal origin from Corsica probably has even coarser particles. The maximum in σ_{rs}, however, need not *per se* be tied to a change in crystallographic or magnetic structure. An alternative explanation is put forward by Lázaro *et al.* (1996) for very fine-grained particles of metallic iron: they showed zero-field cooling curves of iron particles of ~ 1 nm (so called clusters) precipitated in zeolite cavities with a similar maximum which they attributed to blocking of the clusters. Whether their curves are comparable to the present σ_{rs} versus temperature curves is not clear, because no information is given on the maximum field which was imposed on their samples.

The maximum in σ_{rs} may serve as an indicative tool for detecting greigite. The nature of potential changes in physical, crystallographic and magnetic properties through this temperature interval, however, remains to be investigated.

5 CONCLUSIONS AND IMPLICATIONS FOR PALAEOMAGNETIC STUDIES

Synthetic greigite alters chemically on heating. The alteration reactions set in at $\sim 200\,^{\circ}$C. The reaction products depend on the surrounding environment (air or an inert gas), and this precludes direct determination of the Curie temperature of greigite. Synthetic greigite shows the same typical thermomagnetic behaviour in air as noted earlier in natural greigites, and this procedure is recommended to detect greigite. Thermal scans of the initial susceptibility are considerably less diagnostic. When comparing thermal scans of altering material, the specific conditions in the various instruments used should be taken into consideration. For example, differences between thermal scans of the initial susceptibility and thermomagnetic runs—both in air—can be related to the amount of air available to react with the sample. In addition, differences in magnetic behaviour may be caused by differences in purity and/or oxidation of the greigite.

On cooling to 4 K, $(B_0)_c$ and $(B_0)_{cr}$ of greigite do not show discontinuities which could be indicative of a magnetic transition. The present sample material, however, may be insufficiently stoichiometric to reveal a transition. σ_{rs} goes through a broad maximum at ~ 10 K, which hints at a transition. The σ_{rs} maximum is also observed in natural greigite samples that are coarser-grained.

The most important implication for palaeomagnetic studies is that the presence of greigite in a rock should never be based on the analysis of alternating field demagnetization properties alone, because these properties are very similar for greigite and magnetite. Greigite may be inferred from high σ_{rs}/χ_{in} values (Snowball 1991; Roberts 1995; Dekkers & Schoonen 1996; Snowball & Torii 1999) and the occurrence of gyroremanent magnetization (Snowball 1997; Hu *et al.* 1998; Sagnotti & Winkler 1999). These are probably indicators of a dominant single-domain (SD) state, rather than a direct indicator of greigite. A combination of thermal and hysteresis properties yields a set of unambiguous indicators for greigite when it is the dominant magnetic mineral (mixtures of magnetic minerals are quickly dominated magnetically by magnetite): SD-like hysteresis parameters, fairly low stability with respect to alternating fields, and typical alteration behaviour when heated in air in strong-field thermomagnetic runs. The low sensitivity of most Curie balances requires a pre-concentration step in natural samples. Low-temperature measurements could be diagnostic of greigite: this has the advantage of avoiding alteration, but specific instrumentation is required for the cooling to 4 K.

ACKNOWLEDGMENTS

MJD acknowledges the Royal Netherlands Academy of Sciences and Arts for support in the form of a fellowship. The support of the Netherlands Science Foundation (ALW, Earth and Life Sciences Council) to HFP is also gratefully acknowledged. Some of the greigite samples were synthesized in the laboratory of MAAS, which was established with financial support of the State University of New York at Stony Brook. Low-temperature hysteresis measurements were performed with the vibrating sample magnetometer at the Physics Department, Nijmegen University (The Netherlands), with the assistance of Willy Vollenberg. Thermal scans of the initial susceptibility were measured with a CS2 attachment to a Geophysica Brno KLY-2 susceptometer at the Institute for Rock Magnetism (Minneapolis, USA). Comments by Ian Snowball and Andy Roberts substantially improved the manuscript. This study was carried out in the framework of the Vening-Meinesz Research School of Geodynamics.

REFERENCES

Aragón, R., Buttrey, D.J., Shepherd, J.P. & Honig, J.M., 1985. Influence of non-stoichiometry on the Verwey transition, *Phys. Rev.,* **31,** 430–436.

Berner, R.A., 1967. Thermodynamic stability of sedimentary iron sulfides, *Am. J. Sci.,* **265,** 773–785.

Buckey, A.N. & Woods, R., 1985. X-ray photoelectron spectroscopy of oxidized pyrrhotite surfaces. I. Exposure to air, *Appl. Surface Sci.,* **22/23,** 280–287.

Buckey, A.N. & Woods, R., 1987. The surface oxidation of pyrite, *Appl. Surface Sci.,* **27,** 437–452.

Coey, J.M.D., Spender, M.R. & Morrish, A.H., 1970. The magnetic structure of the spinel, Fe_3S_4, *Solid State Comm.,* **8,** 1605–1608.

Collinson, D.W., 1983. *Methods in Rock Magnetism and Palaeomagnetism—Techniques and Instrumentation,* Chapman & Hall, London.

Dekkers, M.J. & Schoonen, M.A.A., 1994. An electrokinetic study of synthetic greigite and pyrrhotite, *Geochim. cosmochim. Acta,* **58,** 4147–4153.

Dekkers, M.J. & Schoonen, M.A.A., 1996. Magnetic properties of hydrothermally synthesized greigite—1. Rock magnetic parameters at room temperature, *Geophys. J. Int.,* **126,** 360–368.

Dekkers, M.J., Mattéi, J.L., Fillion, G. & Rochette, P., 1989. Grain-size dependence of the magnetic behavior of pyrrhotite during its low temperature transition at 34 K, *Geophys. Res. Lett.,* **16,** 855–858.

Fassbinder, J.W.E. & Stanjek, H., 1994. Magnetic properties of biogenic soil greigite (Fe_3S_4), *Geophys. Res. Lett.,* **21,** 2349–2352.

Fillion, G., Mattéi, J.L., Rochette, P. & Wolfers, P., 1992. Neutron study of 4C pyrrhotite, *J. Magn. magn. Mat.,* **104–107,** 1985–1986.

Florindo, F. & Sagnotti, L., 1995. Palaeomagnetism and rock magnetism in the upper Pliocene Valle Ricca (Rome, Italy) section, *Geophys. J. Int.,* **123,** 340–354.

Garrels, R.M. & Christ, C.L., 1965. *Solution, Minerals and Equilibria,* Harper & Row and John Weather Hill, New York.

Graham, J., Bennett, C.E.G. & van Riessen, A., 1987. Oxygen in pyrrhotite: 1. Thermomagnetic behavior and annealing of pyrrhotites containing small quantities of oxygen, *Am. Min.,* **72,** 599–604.

Hallam, D.F. & Maher, B.A., 1994. A record of reversed polarity carried by the iron sulphide greigite in British early Pleistocene sediments, *Earth planet. Sci. Lett.,* **121,** 71–80.

Heywood, B.R., Bazylinski, D.A., Garratt-Reed, A., Mann, S. & Frankel, R.B., 1990. Controlled biosynthesis of greigite (Fe_3S_4) in magnetotactic bacteria, *Naturwissenschaften,* **77,** 536–538.

Hoare, I.C., Hurst, H.J., Stuart, W.I. & White, T.J., 1988. Thermal decomposition of pyrite, *J. Chem. Soc. Faraday Trans.,* **1(84),** 3071–3077.

Horng, C.-S., Chen, J.-C. & Lee, T.-Q., 1992a. Variations in magnetic minerals from two Plio-Pleistocene marine-deposited sections, southwestern Taiwan, *J. geol. Soc. China,* **35,** 323–335.

Horng, C.-S., Laj, C., Lee, T.-Q. & Chen, J.-C., 1992b. Magnetic characteristics of sedimentary rocks from the Tsengwen-chi and Erhjen-chi sections in southwestern Taiwan, *TAO,* **3,** 519–532.

Horng, C.-S., Torii, M., Shea, K.-S. & Kao, S.-J., 1999. Inconsistent magnetic polarities between greigite- and pyrrhotite/magnetite-bearing marine sediments from the Tsailiao-chi section, southwestern Taiwan, *Earth planet. Sci. Lett.,* **164,** 467–481.

Hu, S., Appel, E., Hoffmann, V., Schmahl, W.W. & Wang, S., 1998. Gyromagnetic remanence acquired by greigite (Fe_3S_4) during static three-axis alternating field demagnetization, *Geophys. J. Int.,* **134,** 831–842.

Hunt, C.P., Moskowitz, B.M. & Banerjee, S.K., 1995. Magnetic properties of rocks and minerals, in *Handbook of Physical Constants,* AGU Reference Shelf 3, pp. 189–204, ed. Ahrens, T.J., AGU, Washington.

Jones, C.F., LeCount, S., Smart, R., St. C. & White, T.J., 1992. Compositional and structural alteration of pyrrhotite surfaces in solution: XPS XRD Studies, *Appl. Surface Sci.,* **55,** 65–85.

Knipe, S.W., Mycroft, J.R., Pratt, A.R., Nesbitt, H.W. & Bancroft, G.M., 1995. X-ray photoelectron spectroscopic study of water adsorption on iron sulphide minerals, *Geochim. cosmochim. Acta,* **59,** 1079–1090.

Krs, M., Krsova, M., Pruner, P., Zeman, A., Novak, F. & Jansa, J., 1990. A petromagnetic study of Miocene rocks bearing micro-organic material and the magnetic mineral greigite (Sokolov and Cheb basins, Czechoslovakia), *Phys. Earth planet. Inter.,* **63,** 98–112.

Krs, M., Novak, F., Krsova, M., Pruner, P., Kouklíková, L. & Jansa, J., 1992. Magnetic properties and metastability of greigite-smythite mineralization in brown-coal basins of the Krusné hory Piedmont, Bohemia, *Phys. Earth planet. Inter.,* **70,** 273–287.

Krupp, R.E., 1994. Phase relations and phase transformations between the low-temperature iron sulfides mackinawite, greigite, and smythite, *Eur. J. Min.,* **6,** 265–278.

Lázaro, F.J., García, J.L., Schünemann, V., Butzlaff, Ch., Larrea, A. & Zaluska-Kotur, M.A., 1996. Iron clusters supported in a zeolite matrix: Comparison of different magnetic characterizations, *Phys. Rev. B,* **53,** 13 934–13 941.

Moskowitz, B.M., Frankel, R.B. & Bazylinski, D.A., 1993. Rock magnetic criteria for the detection of biogenic magnetite, *Earth planet. Sci. Lett.,* **120,** 283–300.

Mott, N.F., 1980. Materials with mixed valency that show a Verwey transition, *Phil. Mag. B,* **42,** 32–335.

Mullender, T.A.T., van Velzen, A.J. & Dekkers, M.J., 1993. Continuous drift correction and separate identification of ferrimagnetic and paramagnetic contributions in thermomagnetic runs, *Geophys. J. Int.,* **114,** 663–672.

Mycroft, J.R., Nesbitt, H.W. & Pratt, A.R., 1995. X-ray photon and Auger electron spectroscopy of air-oxidized pyrrhotite: Distribution of oxidized species with depth, *Geochim. cosmochim. Acta,* **59,** 721–733.

Oldfield, F., Darnley, I., Yates, G., France, D.E. & Hilton, J., 1992. Storage diagenesis versus sulphide authigenesis: possible implications in environmental magnetism, *J. Paleolimnol.,* **7,** 179–189.

Özdemir, Ö., Dunlop, D.J. & Moskowitz, B.M., 1993. The effect of oxidation on the Verwey transition in magnetite, *Geophys. Res. Lett.,* **20,** 1671–1674.

Pratt, A.R., Muir, I.J. & Nesbitt, H.W., 1994. X-ray photoelectron and Auger electron spectroscopic studies of pyrrhotite and mechanism of air oxidation, *Geochim. cosmochim. Acta,* **58,** 827–841.

Reynolds, R.L., Tuttle, M.L., Rice, C.A., Fishman, N.S., Karachewski, J.A. & Sherman, D.M., 1994. Magnetization and geochemistry of greigite-bearing Cretaceous strata, North Slope Basin, Alaska, *Am. J. Sci.,* **294,** 485–528.

Roberts, A.P., 1995. Magnetic properties of sedimentary greigite (Fe_3S_4), *Earth planet. Sci. Lett.,* **134,** 227–236.

Roberts, A.P. & Turner, G.M., 1993. Diagenetic formation of ferrimagnetic iron sulphide minerals in rapidly deposited marine sediments, South Island, New Zealand, *Earth planet. Sci. Lett.,* **115,** 257–273.

Roberts, A.P., Reynolds, R.L., Verosub, K.L. & Adam, D.P., 1996. Environmental magnetic implications of greigite (Fe_3S_4) formation in a 3 million year lake sediment record from Butte Valley, Northern California, *Geophys. Res. Lett.,* **23,** 2859–2862.

Roberts, A.P., Stoner, J.S. & Richter, C., 1999. Diagenetic magnetic enhancement of sapropels from the eastern Mediterranean Sea, *Mar. Geol.,* **153,** 103–116.

Rochette, P., Fillion, G., Mattéi, J.L. & Dekkers, M.J., 1990. Magnetic transition at 30–34 Kelvin in pyrrhotite: insight into a widespread occurrence of this mineral in rocks, *Earth planet. Sci. Lett.,* **98,** 319–328.

Sagnotti, L. & Winkler, A., 1999. Rock magnetism and palaeomagnetism of greigite-bearing mudstones in the Italian peninsula, *Earth planet. Sci. Lett.,* **165,** 67–80.

Schwarz, E.J., 1975. Magnetic properties of pyrrhotite and their use in applied geology and geophysics, *Geol. Surv. Paper* 74-59, Geological Survey of Canada, Ottawa.

Schwertmann, U. & Cornell, R.M., 1991. *Iron Oxides in the Laboratory—Preparation and Characterization,* VCH, Weinheim.

Skinner, B.J., Erd, R.C. & Grimaldi, F.S., 1964. Greigite, the thiospinel of iron; a new mineral, *Am. Min.,* **49,** 543–555.

Snowball, I.F., 1991. Magnetic hysteresis properties of greigite (Fe_3S_4) and a new occurrence in Holocene sediments from Swedish Lappland, *Phys. Earth planet. Inter.,* **68,** 32–40.

Snowball, I.F., 1997. The detection of single-domain greigite (Fe_3S_4) using rotational remanent magnetization (RRM) and the effective gyro field (*Bg*): mineral magnetic and palaeomagnetic applications, *Geophys. J. Int.,* **130,** 704–716.

Snowball, I.F. & Thompson, R., 1988. The occurrence of greigite in the sediments of Loch Lomond, *J. Quat. Sci.,* **3,** 121–125.

Snowball, I.F. & Thompson, R., 1990. A stable remanence in Holocene sediments, *J. geophys. Res.,* **95,** 4471–4479.

Snowball, I.F. & Torii, M., 1999. Incidence and significance of ferrimagnetic iron sulphides in Quaternary studies, in *Quaternary Climates and Magnetism,* pp. 199–230, eds Maher, B.A. & Thompson, R., Cambridge University Press, Cambridge.

Spender, M.R., Coey, J.M.D. & Morrish, A.H., 1972. The magnetic properties and Mössbauer spectra of synthetic samples of Fe_3S_4, *Can. J. Phys.,* **50,** 2313–2326.

Taylor, L.A., 1970. Low temperature phase relations in the Fe-S system, *Carnegie Inst. Wash. Yearbook,* **69,** 259–270.

Taylor, L.A. & Mao, H.K., 1971. Observations on the occurrence and stability of smythite, $Fe_{3.25}S_4$, *Carnegie Inst. Wash. Yearbook,* **70,** 290–291.

Torii, M., Fukuma, K., Horng, C.-S. & Lee, T.-Q., 1996. Magnetic discrimination of pyrrhotite- and greigite-bearing sediment samples, *Geophys. Res. Lett.,* **22,** 1813–1816.

Van den Berghe, R.E., de Grave, E., de Bakker, P.M.A., Krs, M. & Hus, J.J., 1991. Mössbauer effect study of natural greigite, *Hyperfine Interact.,* **68,** 319–322.

Vaughan, D.J. & Craig, J.R., 1976. *Mineral Chemistry of Metal Surfaces,* Cambridge University Press, Cambridge.

Vaughan, D.J. & Craig, J.R., 1985. The crystal chemistry of iron-nickel thiospinels, *Am. Min.,* **70,** 1036–1043.

Vaughan, D.J. & Tossell, J.A., 1981. Electronic structure of thiospinel minerals: results from MO calculations, *Am. Min.,* **66,** 1250–1253.